photonics

MDPI

Communication

Differentially Fed, Wideband Dual-Polarized Filtering Dielectric Resonator Patch Antenna Using a Sequentially Rotated Shorting Coupling Structure

Haitao Song [1,*], Baoxing Duan [1] and Feifei Zhang [2]

[1] School of Microelectronics, Xidian University, Xi'an 710071, China
[2] National Research Institute of Radio Spectrum Management, Xi'an 710071, China
* Correspondence: xidiansonght@126.com

Abstract: A wideband dual-polarized dielectric resonator antenna (DRA) with gain-filtering response was proposed in this paper. First, a differentially fed, low-profile crossed-DRA was used to obtain orthogonal polarizations with two resonant modes. A radiation null at upper band edge was also generalized. Second, with the introduction of four parasitic patches at the top of the crossed DRA, another resonant mode at lower band was excited, and the bandwidth was greatly expanded. Moreover, the introduction of parasitic patches could also help improve the selectivity of realized gain with another radiation null at the upper band edge. Furthermore, four sequentially rotated shorting coupling structures (SRSCSs) were proposed for the first time to generalize two additional radiation nulls. Finally, a wideband bandpass filtering response of the realized gain with four radiation nulls was obtained. Prototypes of the proposed antennas were fabricated, and the testing results showed that the antenna had a wide operation band of 57.1% from 2.75 GHz to 4.95 GHz with sharp roll-off at the band edge. This technique could also be used in wireless communication devices at millimeter/optical front ends and other multi-wavelength fiber lasers with micro structures.

Keywords: dielectric resonator antenna; differential antenna; dual-polarized antenna; filtering antenna; micro structure; multi-wavelength fiber laser; optical antenna; wideband antenna

check for updates

Received: 9 February 2025
Revised: 15 February 2025
Accepted: 17 February 2025
Published: 6 March 2025

Citation: Song, H.; Duan, B.; Zhang, F. Differentially Fed, Wideband Dual-Polarized Filtering Dielectric Resonator Patch Antenna Using a Sequentially Rotated Shorting Coupling Structure. *Photonics* **2025**, *12*, 239. https://doi.org/10.3390/photonics12030239

Copyright: © 2025 by the authors. Licensee MDPI, Basel, Switzerland. This article is an open access article distributed under the terms and conditions of the Creative Commons Attribution (CC BY) license (https://creativecommons.org/licenses/by/4.0/).

1. Introduction

Owing to the advantages of large channel capacity and suppression of the multipath-fading effect, wideband dual-polarized antennas were widely used in modern wireless communication systems [1–3], such as base stations and optical front ends. In dual-polarized antenna designs, more functions were demanded with the communication technologies improvement and consumer demand growth, such as more compact sizes, higher isolation levels and lower cross-polarizations. Among these demands, the higher selectivity of the wireless communication system has become one of the most urgent problems to be solved. As the electromagnetic environments grow worse with the miniaturization of wireless devices, antennas in multi-band systems need to be isolated with each other. Thus, antennas with gain-filtering responses have become promising candidates to solve this problem.

To obtain the filtering response of the realized gain, filtering structures were mostly introduced into feeding structures of antennas [4–12]. Some of them were coupled resonator filtering structures [4–9], and the others have a similar type to stepped impedance resonators [10–12]. In these designs, the antennas generally act as the last stage of filters,

and the electromagnetic energy outside the passband could hardly get through feedlines. Thus, radiation gain could be well suppressed outside the operation band of antennas. However, the introduction of filters brings non-ignorable insertion loss, especially in the millimeter waveband. Meanwhile, extra spaces were needed to place filtering feeding structures. In recent years, gain-filtering responses obtained without filtering circuits have also been reported in some of the literatures [13–18]. In these designs, inherent resonant characteristics of antennas have been investigated to generate filtering responses of the realized gain. For example, by loading parasitic patches of different types in [13], electrical and magnetic gap coupling could be generated between the radiator and parasitic patches, and the operation bandwidth was enhanced with two radiation nulls besides the parasitic frequencies. In [14], a dual-polarized patch antenna was proposed with wideband bandpass gain-filtering response. The two radiation nulls were produced by a square loop and a cross loop, respectively. Except for this, radiation nulls could also be obtained by etching open slots on radiators [15], loading E-shaped slots and shorting pins on radiators with stacked patches [16], using defected ground structures (DGS), cross slot and shorting pins [17], as well as defected microstrip structure [18].

Among the above designs, the antennas usually have only two radiation nulls, especially in dual-polarized filtering antenna designs. And this was not enough in practical applications. To obtain a better gain-suppression level outside the operation band, more radiation nulls were demanded. In view of this, this paper presents a wideband dual-polarized filtering antenna with four radiation nulls. As DRA has the advantages of a compact size, a wide operation band, and an explicit physical meaning [19,20], a thin crossed DRA differentially fed by extended coaxial probes was proposed with two resonances. With the introduction of four parasitic patches around the DRA, another resonance occurred. The operation bandwidth and radiation gain were further enhanced, which had similar functions with [21]. Meanwhile, the parasitic patches offered two radiation nulls at the upper band edge. To obtain a good wideband bandpass gain-filtering response, four SRSCS were introduced. A basic null was generated at the lower band edge, as well as a third-order null at the upper band edge. Finally, the proposed antenna performed a good bandpass gain-filtering response with four radiation nulls. The SRSCS was printed at the same layer with four parasitic patches, so the overall structure of the proposed antenna was relatively easy for fabrication. Measured results of the two prototypes showed that the proposed antenna had a wide operation band of 57.1% from 2.75 GHz to 4.95 GHz for VSWR < 2. An average gain of 7.5 dBi across the operation band was also obtained with four radiation nulls.

Organization of this paper is as follows: the antenna configuration and detailed working mechanism are discussed in Section 2. The measured results for the proposed antenna and discussions are illustrated in Section 3. The conclusion is presented in Section 4.

2. Antenna Design Process and Analysis

Configuration of the proposed differentially fed dual-linearly polarized DRA was illustrated in Figure 1. The proposed antenna consists of a cross-DRA with relative permittivity of 9.21, four square parasitic patches, four SRSCSs, and an F4B substrate with relative permittivity of 2.65 and thickness of 0.5 mm. The crossed DRA was differentially fed by two pairs of coaxial cables. When port 1 and port 2 were differentially fed, vertical polarization could be realized for the proposed antenna. When port 3 and port 4 were differentially fed, horizonal polarization was obtained. The detailed working principle of the proposed antenna was illustrated in the following sections.

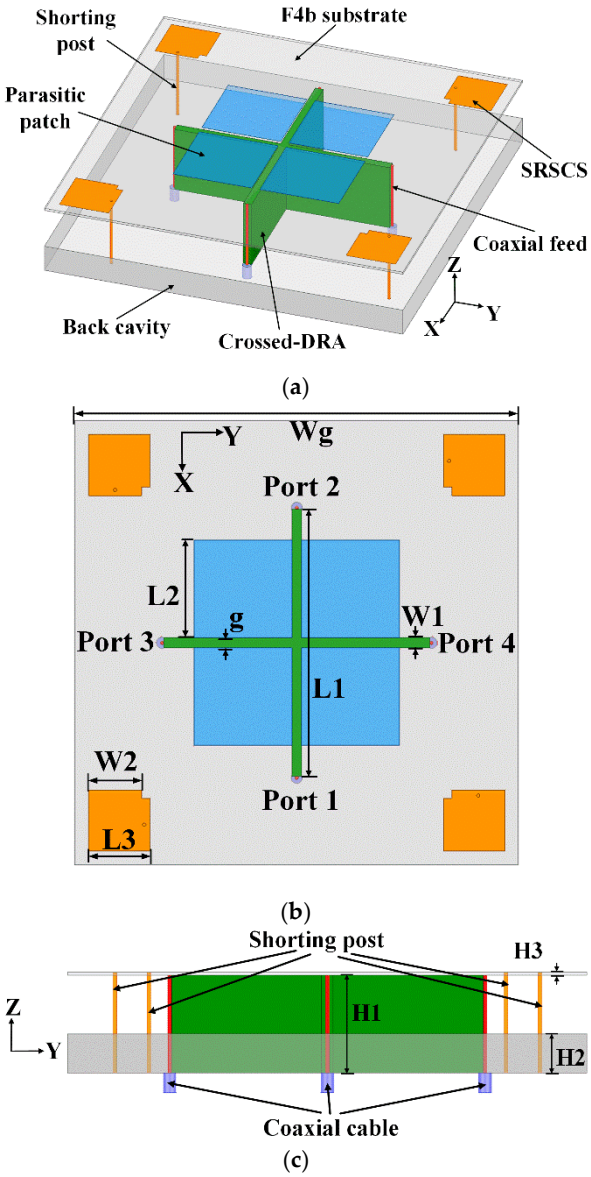

Figure 1. Configuration of the proposed antenna: (**a**) perspective view, (**b**) top view, (**c**) front view. The optimized parameters are as follows (unit: mm): Wg = 80.0, W1 = 1.8, W2 = 9.5, L1 = 48.0, L2 = 17.6, L3 = 11.0, H1 = 15.0, H2 = 6.0, H3 = 0.5, g = 1.8.

An evolution process was investigated to elaborate the working mechanism of the proposed antenna, as Figure 2a shows. Ant.1 was a crossed DRA differentially by coaxial cables, and Ant.2 was four-printed square parasitic patches loading on the top of Ant.1. Ant.3 was a back cavity added to Ant.2. The antenna in the final design was four SRSCSs added to Ant.3. The detailed working mechanism for generating four radiation nulls were as follows:

(1) Reference Antenna 1

As can be seen in Figure 2, a thin crossed DRA(Ant.1) was proposed with a length of 48 mm, a height of 15 mm, and a thickness of 1.8 mm. The differential VSWR and realized gain of Ant.1 were illustrated in Figure 2b when port 1 and port 2 were differentially fed. The crossed DRA resonances were at about 3.5 GHz and 4.8 GHz. Electric fields for Ant.1 at the four frequencies were plotted in Figure 3. The electric length along x-axis was about half a wavelength at 4.8 GHz, while it was shorter than half a wavelength at 3.5 GHz. Thus, f_1 changed little with L1, and f_2 moved to the lower band as L1 increased, as could be

seen in Figure 4a. On the other hand, the electric length of the first resonant mode grew longer, and f_1 moved to the lower band significantly when the H1 of Ant.1 grew longer in Figure 4b, which was similar to the constraint condition of width and height in waveguide theory.

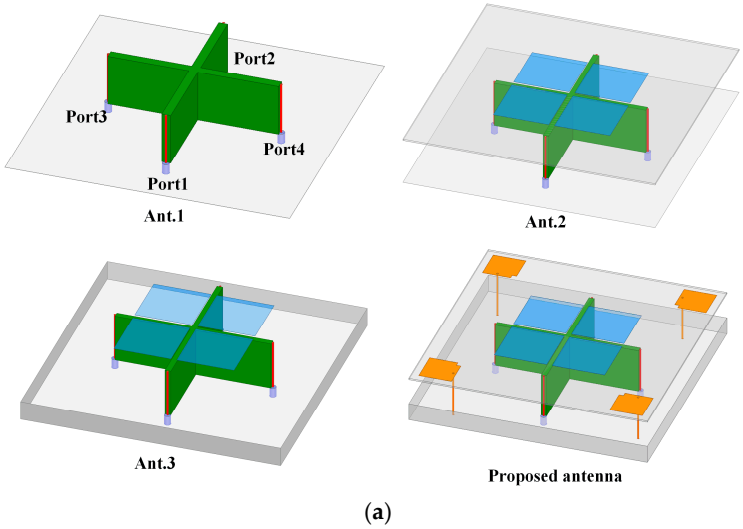

(**a**)

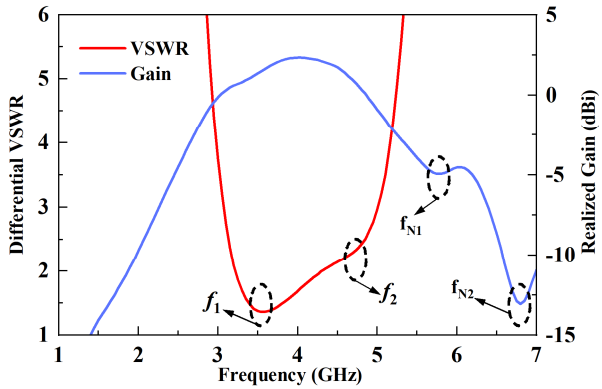

(**b**)

Figure 2. (**a**) Evolution process of the antenna and (**b**) Simulation results for Ant.1.

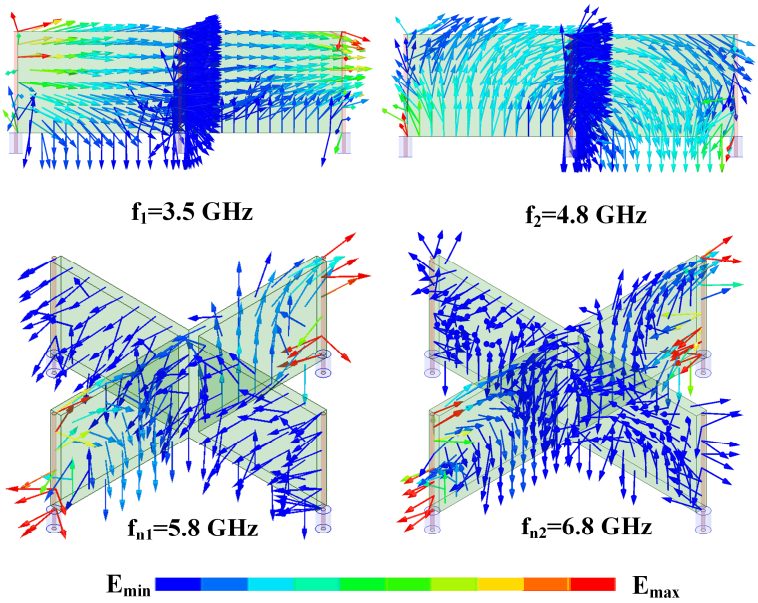

Figure 3. Electric fields for Ant.1 at the resonant frequencies and radiation nulls.

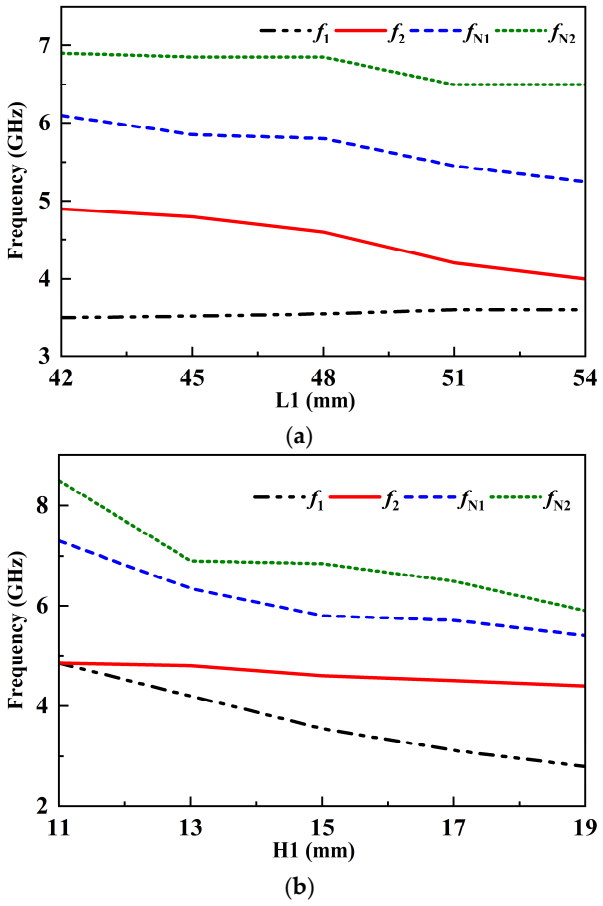

Figure 4. Resonant Frequencies and radiation nulls of Ant.1 vary with (**a**) L1 and (**b**) H1.

It could be seen from Figure 2b that two inherent radiation nulls were obtained outside the upper band at about 5.8 GHz and 6.8 GHz. First, the resonant characteristic was poor outside the operation band, which indicates week radiation performance at the two frequencies. Second, the electric fields were inverse about the z-axis at the two radiation nulls, as illustrated in Figure 3, which contributed to worse radiation performance in the main radiation direction. Thus, the two radiation nulls were obtained. The parameter study carried out in Figure 4 shows that the two radiation nulls moved to the lower bands as L1 or H1 increased, which was similar to trends of the two resonant modes.

(2) Reference Antenna 2 and Antenna 3

The crossed DRA(Ant.1) suffered from low in-band gain and poor out-band gain-suppression levels in Figure 2. In view of this, four square patches were introduced on the top of DRA, as Figure 5 shows. The resonant characteristics and realized gains for Ant.2 were also illustrated in Figure 5. Another resonance at about 2.8 GHz was generated by the square patches. Here, the patches acted as parasitic structures, as well as directors, and the radiation gain increases at the operation band. Moreover, owing to the coupling effect, the two radiation nulls move to lower bands. A back cavity was loaded on the metal ground for better impedance matching performance (Ant.3). At the same time, the realized gain outside the upper band for Ant.3 was suppressed further. Figure 6 shows current distributions on the radiating patches at the frequencies of the two radiation nulls. First, the resonant characteristics of patches were weak at the frequencies of the two nulls. Meanwhile, dominant currents distributed along the x-axis were symmetrical, which resulted in worse radiating performance in the main radiation direction. As a result, deep roll-off could be observed at the two radiation nulls. A parameter study on the realized

gain for Ant.3 was performed to show the influence of patch size on radiation nulls, as shown in Figure 7. It could be seen that the two radiation nulls move to lower bands as L2 increased. At the same time, the realized gains of Null1 grew higher as it became closer to resonant frequency band. As last, a medium value of 17.6 mm was chosen for compromise.

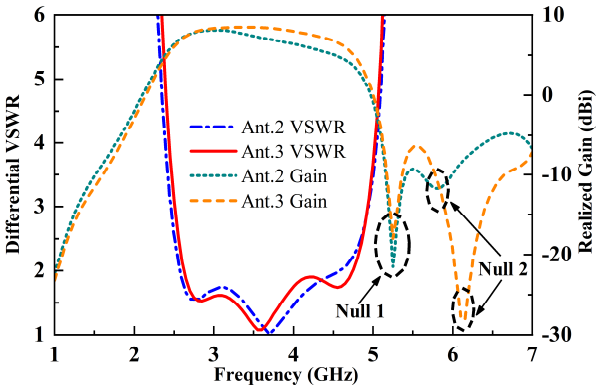

Figure 5. Simulated differential VSWR and realized gain for Ant.2 and Ant.3.

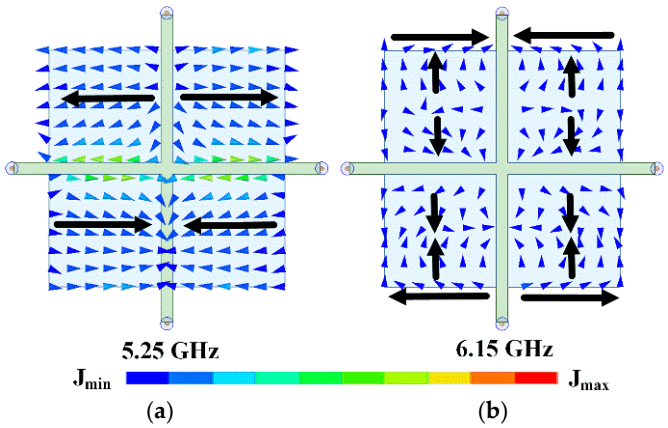

Figure 6. Current distributions on the square patches of Ant.3 at the two radiation nulls: (**a**) 5.25 GHz and (**b**) 6.15 GHz.

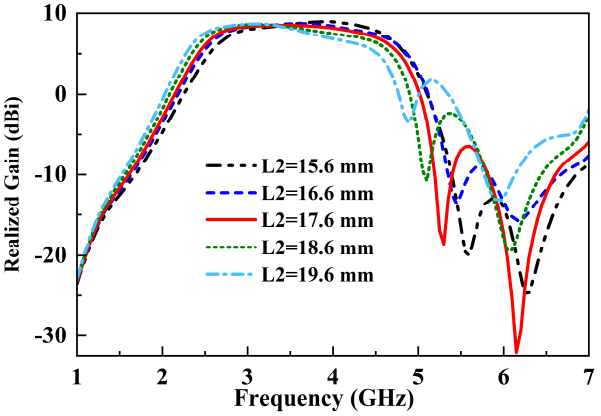

Figure 7. The realized gain of Ant.3 varied with L2.

(3) The proposed antenna

To obtain better gain-suppression performance, four SRSCSs were introduced, offering two additional radiation nulls at 1.85 GHz and 6.7 GHz, as shown in Figure 8. As the SRSCSs did not operate not as radiators, impedance matching performance of the antenna was almost unaffected. For a better understanding the function of the SRSCS, the current

distributions on the antenna at the frequencies of the two radiation nulls were illustrated in Figure 9. First, currents on the radiating patched were totally inverse with the SRSCS along XOY plane at 1.85 GHz, which contributes to a radiation null in the main radiation direction. Second, the current length of each SRSCS was about a quarter wave length, which could be used to determine the frequency of the radiation null. Also, the currents on the radiating patch and SRSCS were inverse at 6.7 GHz, and the current length of each SRSCS was about a three-quarter wave length. Thus, when the length of the SRSCS was fixed, the two radiation nulls were determined.

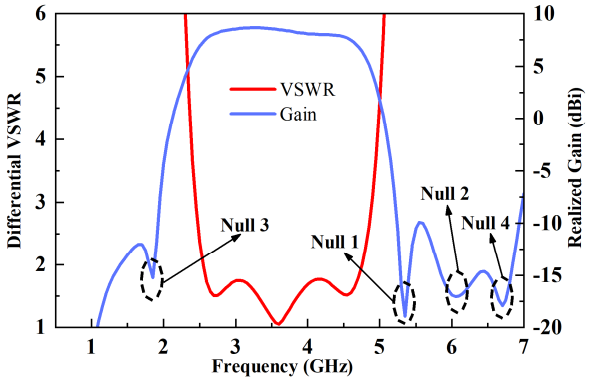

Figure 8. Differential VSWR and realized gain for the proposed antenna.

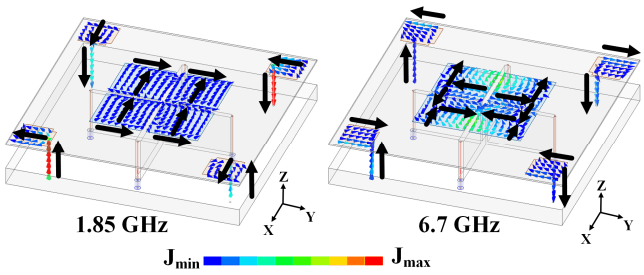

Figure 9. Current distributions on the antenna at 1.85 GHz and 6.7 GHz.

A parameter study was also carried out to show the influence of the SRSCS on the radiation nulls of the proposed antenna, as Figure 10 shows. When the length of the horizontal patch of the SRSCS increases, radiation null 3 moved to lower frequency band, and radiation null4 moved to lower frequency band. Meanwhile, the other two radiation nulls remained unchanged. Finally, the proposed antenna had a wide operation band from 2.55 GHz to 4.75 GHz for VSWR < 2. And the realized gain at the operation band was 7.7 ± 0.7 dBi, with four radiation nulls at 1.85 GHz, 5.35 GHz, 6.05 GHz and 6.7 GHz.

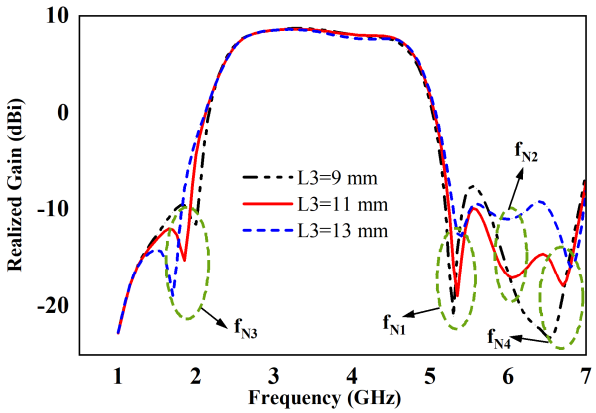

Figure 10. Realized gain for Ant.3 varied with width of the CDR.

3. Experimental Results and Discussion

A prototype of the proposed antenna was fabricated and tested, as Figure 11 shows. Two pairs of power dividers were also used to feed the differential ports. The measured VSWR and realized gains were shown in Figure 12, as well as the port isolation level. The measured radiation patterns at different frequencies were illustrated in Figure 13. The measured results showed that the proposed antenna had a wide operation band from 2.75 GHz to 4.95 GHz for VSWR < 2. The reason for the frequency shift of the measured results was mainly due to fabrication and testing errors. The radiation gain at the operation band varied from 6.8 dBi to 8.2 dBi. Also, four radiation nulls were observed at 1.35 GHz, 2.15 GHz, 5.65 GHz and 6.4 GHz, which shows a good gain-filtering response across the operation band. High port isolation levels of better than 37.5 dB were also obtained. Moreover, the radiation patterns at 3.3 GHz and 4.2 GHz also showed good unidirectional radiation of the proposed antenna.

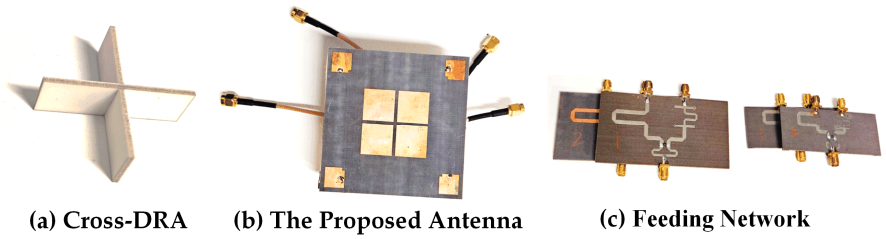

Figure 11. The fabricated prototype: (**a**) crossed DRA, (**b**) the fabricated antenna and (**c**) the feeding network.

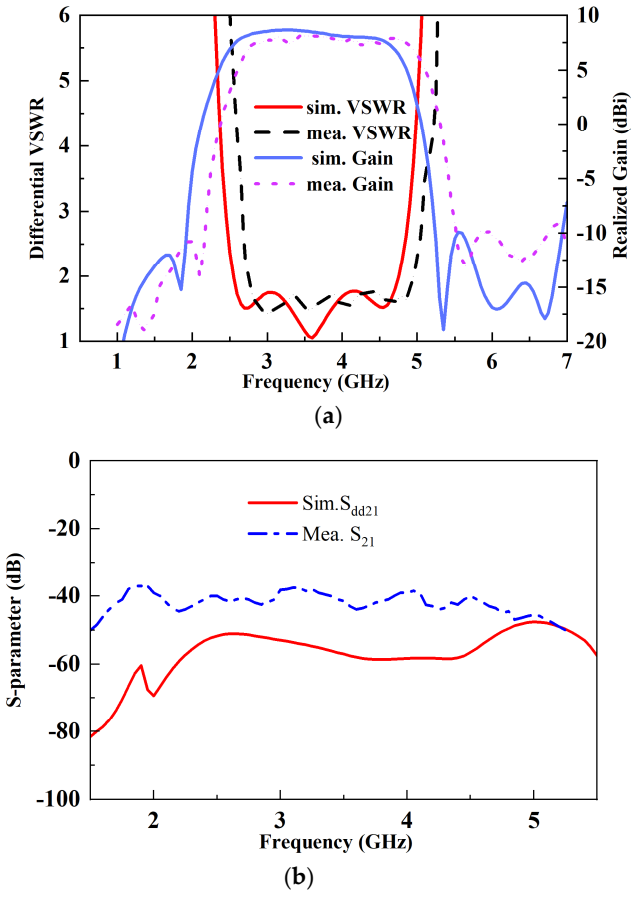

Figure 12. Simulated and measured (**a**) VSWR and realized gains, (**b**) S_{21} of the proposed antenna.

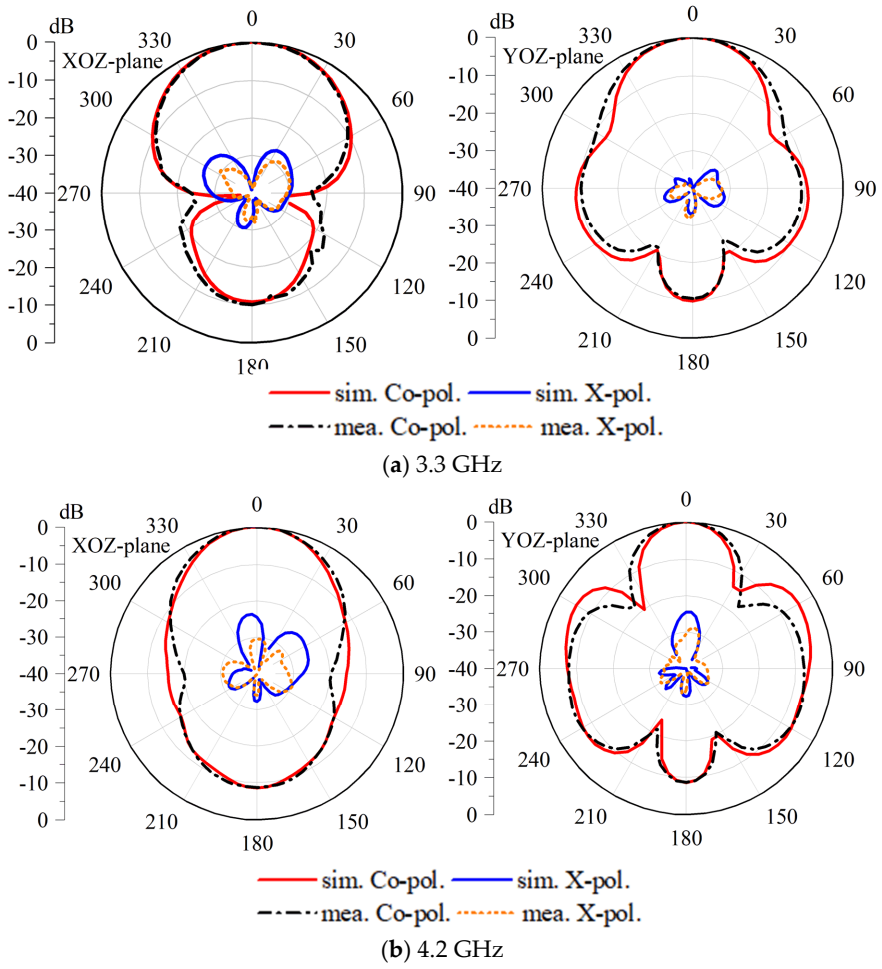

(**a**) 3.3 GHz

(**b**) 4.2 GHz

Figure 13. Simulated and measured radiation patterns of the antenna at different frequencies.

A comparison was made between the proposed antenna and the reference antennas in literature, as shown in Table 1. It could be seen that the proposed antenna has a wider bandwidth than the other antennas. With the introduction of SRSCS, more radiation nulls were introduced, which contributes to a wide bandpass filtering response of the radiation gain. Thus, the filtering performance was better than the other references. Although the antenna in [12,15] have a more compact size, the single polarizations reduce their applicability in complex environments. As a contrast, the proposed antenna shows good performance in bandwidth, filtering performance, as well as practicality.

Table 1. Comparison of relevant antennas.

Ref.	Radiator Size (λ_c)	Bandwidth	Polarization	Radiation Nulls
[9]	0.36 × 0.36 × 0.06	9.9%	VP/HP	2
[11]	0.49 × 0.49 × 0.13	12.3%/7.6%	±45°/±45°	3
[12]	0.6 × 0.6 × 0.095	21.3%	LP	2
[14]	0.37 × 0.37 × 0.23	48.7%	±45°	2
[15]	0.35 × 0.24 × 0.027	7%	LP	2
Pro.	0.616 × 0.616 × 0.199	57.1%	VP/HP	4

4. Conclusions

In this paper, a differentially fed, wideband dual-polarized filtering antenna was proposed. The proposed SRSCS provides not only a wider operation band, but also gain-

filtering response. The testing results show that the antenna had a wide operation band of 57.1% from 2.75 GHz to 4.95 GHz with sharp roll-off at the band edge. Moreover, the structure was simple and easy fabricated. Also, the crossed dielectric resonator had a stable physical structure and low cost. Thus, this technique could be used in wireless communication devices at microwave or optical front ends and other multi-wavelength fiber lasers with micro structures.

Author Contributions: Methodology, H.S. and B.D.; fabrication and testing, F.Z.; writing—original draft preparation, H.S. and F.Z. All authors have read and agreed to the published version of the manuscript.

Funding: This research received no external funding.

Institutional Review Board Statement: Not applicable.

Informed Consent Statement: Not applicable.

Data Availability Statement: All data have been included in the study.

Conflicts of Interest: The authors declare no conflicts of interest.

References

1. Xu, H.-X.; Wang, S.; Wang, C.; Wang, M.; Wang, Y.; Peng, Q. Polarization-Insensitive Metalens and Its Applications to Reflectarrays with Polarization Diversity. *IEEE Trans. Antennas Propag.* **2022**, *70*, 1895–1905. [CrossRef]
2. Cui, Y.; Gao, X.; Li, R. A Broadband Differentially-Fed Dual-Polarized Planar Antenna. *IEEE Trans. Antennas Propag.* **2017**, *65*, 3231–3234. [CrossRef]
3. Wen, D.L.; Zheng, D.Z.; Chu, Q.X. A Wideband Differentially-Fed Dual-Polarized Antenna with Stable Radiation Pattern for Base Stations. *IEEE Trans. Antennas Propag.* **2017**, *65*, 2248–2255. [CrossRef]
4. Mao, C.X.; Gao, S.; Wang, Y.; Luo, Q.; Chu, Q.X. A Shared-Aperture Dual-Band Dual-Polarized Filtering-Antenna-Array with Improved Frequency Response. *IEEE Trans. Antennas Propag.* **2017**, *65*, 1836–1844. [CrossRef]
5. Li, L.; Xiong, H.D.; Wu, W.Y.; Fu, A.B.; Han, J.Y. A T-Shaped Strips Loaded Wideband Filtering Patch Antenna with High Selectivity. *IEEE Antennas Wirel. Propag. Lett.* **2024**, *23*, 89–93. [CrossRef]
6. Wu, R.; Wen, G.H.; Chen, F.C.; Li, J.F.; Ye, L.H.; Cao, W.P. A Low-Profile Broadband Filtering Antenna and Its Array for 5G Applications. *IEEE Antennas Wirel. Propag. Lett.* **2024**, *23*, 2920–2924. [CrossRef]
7. Wu, Q.-S.; Zhang, X.; Zhu, L. Co-Design of a Wideband Circularly Polarized Filtering Patch Antenna with Three Minima in Axial Ratio Response. *IEEE Trans. Antennas Propag.* **2018**, *66*, 5022–5030. [CrossRef]
8. Guo, J.; Chen, Y.; Yang, D.; Sun, K.; Pan, J.; Liu, S. Design of Wideband Filtering Patch Antenna Array with High Aperture Efficiency and Good Filtering Performance. *IEEE Trans. Antennas Propag.* **2024**, *72*, 974–979. [CrossRef]
9. Tang, H.; Chen, J.; Yang, W.; Zhou, L.; Li, W. Differential Dual-Band Dual-Polarized Dielectric Resonator Antenna. *IEEE Trans. Antennas Propag.* **2017**, *65*, 855–860. [CrossRef]
10. Li, D.; Yang, C.; Shi, L.; Liu, Y.; Chen, Q.; Shinohara, N. A High-Gain Filtering Quasi-Yagi Antenna Based on Compressed Third-Order Mode Dipole. *IEEE Antennas Wirel. Propag. Lett.* **2024**, *23*, 2860–2864. [CrossRef]
11. Li, Y.; Zhao, Z.; Tang, Z.; Yin, Y. Differentially Fed, Dual-Band Dual-Polarized Filtering Antenna with High Selectivity for 5G Sub-6 GHz Base Station Applications. *IEEE Trans. Antennas Propag.* **2020**, *68*, 3231–3236. [CrossRef]
12. Hu, P.F.; Pan, Y.M.; Zhang, X.Y.; Hu, B.-J. A Filtering Patch Antenna with Reconfigurable Frequency and Bandwidth Using F-Shaped Probe. *IEEE Trans. Antennas Propag.* **2019**, *67*, 121–130. [CrossRef]
13. Qian, J.-F.; Chen, F.-C.; Chu, Q.-X.; Xue, Q.; Lancaster, M.J. A Novel Electric and Magnetic Gap-Coupled Broadband Patch Antenna with Improved Selectivity and Its Application in MIMO System. *IEEE Trans. Antennas Propag.* **2018**, *66*, 5625–5629. [CrossRef]
14. Ding, C.F.; Zhang, X.Y.; Zhang, Y.; Pan, Y.M.; Xue, Q. Compact Broadband Dual-Polarized Filtering Dipole Antenna with High Selectivity for Base-Station Applications. *IEEE Trans. Antennas Propag.* **2018**, *66*, 5747–5756. [CrossRef]
15. Jin, J.Y.; Liao, S.; Xue, Q. Design of Filtering-Radiating Patch Antennas with Tunable Radiation Nulls for High Selectivity. *IEEE Trans. Antennas Propag.* **2018**, *66*, 2125–2130. [CrossRef]
16. Zhang, Y.; Zhang, X.Y.; Ye, L.-H.; Pan, Y.-M. Dual-Band Base Station Array Using Filtering Antenna Elements for Mutual Coupling Suppression. *IEEE Trans. Antennas Propag.* **2016**, *64*, 3423–3430. [CrossRef]
17. Yang, W.; Xun, M.; Che, W.; Feng, W.; Zhang, Y.; Xue, Q. Novel Compact High-Gain Differential-Fed Dual-Polarized Filtering Patch Antenna. *IEEE Trans. Antennas Propag.* **2019**, *67*, 7261–7271. [CrossRef]

18. Liu, Y.-T.; Leung, K.W.; Yang, N. Compact Absorptive Filtering Patch Antenna. *IEEE Trans. Antennas Propag.* **2020**, *68*, 633–642. [CrossRef]
19. Fang, X.S.; Shi, K.P.; Sun, Y.X. Design of the Single-/Dual-Port Wideband Differential Dielectric Resonator Antenna Using Higher Order Mode. *IEEE Antennas Wirel. Propag. Lett.* **2020**, *19*, 1605–1609. [CrossRef]
20. Wang, X.-Y.; Tang, S.-C.; Yang, L.-L.; Chen, J.-X. Differential-Fed Dual-Polarized Dielectric Patch Antenna with Gain Enhancement Based on Higher Order Modes. *IEEE Antennas Wirel. Propag. Lett.* **2020**, *19*, 502–506. [CrossRef]
21. Xu, H.X.; Wang, G.M.; Qi, M.Q.; Zhang, C.X.; Liang, J.G.; Gong, J.Q.; Zhou, Y.C. Analysis and Design of Two-Dimensional Resonant-Type Composite Right/Left-Handed Transmission Lines with Compact Gain-Enhanced Resonant Antennas. *IEEE Trans. Antennas Propag.* **2013**, *61*, 735–747. [CrossRef]

Disclaimer/Publisher's Note: The statements, opinions and data contained in all publications are solely those of the individual author(s) and contributor(s) and not of MDPI and/or the editor(s). MDPI and/or the editor(s) disclaim responsibility for any injury to people or property resulting from any ideas, methods, instructions or products referred to in the content.